Journal of ELECTRONIC MATERIALS, Vol. 46, No. 7, 2017
DOI: 10.1007/s11664-017-5437-5

Effect of Secondary Doping Using Sorbitol on Structure and Transport Properties of PEDOT–PSS Thin Films

SYED KHASIM ,[1,2,7] APSAR PASHA,[2,3] AASHISH S. ROY,[4] AMEENA PARVEEN,[5] and NACER BADI[1,6]

1.—Department of Physics, Faculty of Science, University of Tabuk, Tabuk 71491, Kingdom of Saudi Arabia. 2.—Department of Physics, PESIT-Bangalore South Campus, Bangalore 560100, India. 3.—Department of Physics, Gousia College, Ramnagar, Karnataka 562159, India. 4.—Industrial Chemistry Department, Addis Ababa Science and Technology University, 16417 Addis Ababa, Ethiopia. 5.—Department of Physics, Government First Grade College, Gurmitkal 585124, India. 6.—Center for Advanced Materials, University of Houston, Houston, TX 77204-5004, USA. 7.—e-mail: syed.pes@gmail.com

Poly(3,4-ethylene dioxythiophene):poly(styrenesulphonate) (PEDOT–PSS) in the recent past has emerged as one of the most fascinating conducting polymers for many device applications. The unique feature of PEDOT–PSS is its transparency in the entire visible spectrum with excellent thermal stability. The PEDOT–PSS as prepared as an aqueous dispersion has very low conductivity, and it hinders the performance of a device. In this work we report the conductivity enhancement of PEDOT–PSS thin films through secondary doping using a polar organic solvent such as sorbitol. The mechanism of conductivity enhancement was studied through various physical and chemical characterizations. The effect of sorbitol concentration on structure and transport properties of PEDOT–PSS thin films was investigated in detail. The structural and morphological modifications in PEDOT–PSS due to the addition of sorbitol was studied through Fourier transform spectroscopy, Ultra Violet–visible spectroscopy, theromogravimetric analysis, scanning electron microscopy and atomic force microscopy. The interactions resulting from conformational changes of PEDOT chains that changes from coiled to linear structure due to the sorbitol treatment significantly improves the conductivity of PEDOT–PSS films. The secondary doping of sorbitol reduces the energy barrier that facilitates the charge carrier hopping leading to enhanced conductivity. We have observed that the conductivity of PEDOT–PSS thin films was increased by two fold due to sorbitol treatment when compared to conductivity of pure PEDOT–PSS. We have carried out detailed analysis of dielectric parameters of sorbitol-treated PEDOT–PSS films and found that sorbitol treatment has a significant effect on various dielectric attributes of PEDOT–PSS films. Hence, secondary doping using sorbitol could be a useful way to effectively tailor the conductivity and dielectric properties of PEDOT–PSS thin films that can be used as flexible electrodes in optoelectronic devices.

Key words: PEDOT–PSS, sorbitol, secondary doping, conductivity, thin film devices

INTRODUCTION

In the recent past organic electronic devices have attracted the attention of many researchers all over the world due to their easy processability over large areas; their electronic properties can be easily tuned

(Received November 9, 2016; accepted March 2, 2017; published online March 15, 2017)

by doping organic or inorganic compounds and are compatible with flexible and low weight substrates.[1,2] These organic electronic devices are extensively being used in many applications such as light emitting diodes, organic solar cells, organic field effect transistors,[3–5] bioelectronics and coupling of devices through conducting polymers with biological systems.[6]

Among a number of conducting polymers, poly(3,4-ethylene dioxythiophene):poly(styrene sulphonate) (PEDOT–PSS) in aqueous solutions have drawn more attention mainly due to their superior transparency over the visible range, processability and thermal stability. The[7,8] PEDOT–PSS films in various forms have been used as hole transporting layers in OLED's,[9–11] they have been used as a buffer layer/active layer between ITO in organic solar cells.[12–14] However, these PEDOT–PSS films prepared through aqueous dispersions suffer due to poor conductivity[15,16] which is typically as low as 1 S/Cm,[17,18] this affects and hinders the performance of many of the electronic devices.[19,20]

Much attention is being paid in the recent past to improve the conductivity of PEDOT–PSS by treating with organic solvents[21,22] through secondary doping or due to the addition of small amount fillers.[23] It is found that addition of polar solvents such as dimethyl sulfoxide (DMSO), dimethyl formaldehyde (DMF) and glycerol to PEDOT–PSS significantly affects the conductivity of the films due to the interaction of polar solvents with the polymer chain that induces conformational changes in the PEDOT chain from coiled structure to linear structure. After secondary doping with polar solvents, the electrical conductivity of this transparent PEDOT–PSS is sufficient to be used as a transparent electrode material in many organic electronics.[24]

Sorbitol, being one of the excellent conductive additive/secondary dopant/plasticizers for PEDOT–PSS, can improve the conductivity of PEDOT–PSS films by several orders of magnitude.[25] The reasons for the remarkable change in the conductivity due to sorbitol addition is still under debate.[15,26,27] Hence, much attention is being paid to understand the conductivity enhancement in these systems by understanding the structural and morphological changes occurring due to secondary doping of sorbitol.

In this present work the authors report the effect of secondary doping by using a polar solvent such as sorbitol by mixing it with PEDOT–PSS in different concentrations. The PEDOT–PSS/sorbitol blends in different concentrations were processed into thin films by the spin coating technique. The processed films were characterized by FTIR, ultra violet–visible (UV–Vis) spectra and scanning electron microscopy (SEM) to understand the morphological and structural changes of pristine PEDOT–PSS films. In depth transport studies were carried out through various measurements such as DC/AC conductivities and impedance/dielectric behaviors. Through our studies we have observed a threefold increase in the conductivities of PEDOT–PSS due to the addition of sorbitol in various concentrations. We have also tried to draw an analogy between the changes in conductivities with that of observed morphological/structural changes of pristine PEDOT–PSS due to secondary doping using sorbitol. In comparison with the reports available in the literature on transport properties of sorbitol doped PEDOT–PSS films, in this work, the effect of sorbitol concentration on a vast number of electrical transport parameters were analyzed in depth.

EXPERIMENTAL

Materials and Chemicals

The glass slides coated with ITO of surface resistivity 8–12 Ω/Sq were procured from Sigma Aldrich (India). PEDOT–PSS (Product Code: 483095, Conductive grade with 0.5 wt.% of PEDOT and 0.8 wt.% of PSS in water) and Sorbitol (99.9% purity) were also procured from Sigma-Aldrich (India) and were used as received.

Fabrication of Sorbitol Treated PEDOT–PSS Thin Films

The ITO-coated glass substrates of dimension 2.5×2.5 cm^2 were cleaned with acetone, IPA and deionized (DI) water and dried under dynamic vacuum prior to use. The aqueous solution of PEDOT–PSS was then post treated with sorbitol at different wt.% such as 5 wt.%, 10 wt.%, 15 wt.%, and 20 wt.% of sorbitol in PEDOT–PSS, and the solutions were sonicated in the ultra-sonication bath for 1 h at room temperature to obtain the homogeneous dispersion. Pristine PEDOT–PSS thin films and PEDOT–PSS films treated with sorbitol were spin coated over ITO-coated glass substrates at 1000 rpm using the spin coating unit (spin NXG-P1). The deposited films were further dried in dynamic vacuum at 120°C to remove the water content from the film.

Characterization of PEDOT–PSS Films

The structural characterization of spin-coated PEDOT–PSS and PEDOT–PSS treated with sorbitol films were studied through FTIR technique using a FTIR spectrometer (Thermo-Nocolet 6700) in KBr medium. The morphological studies of the surface in these thin films were studied through a scanning electron microscope (Zeiss Ultra 60) and an atomic force microscope (AFM, Bruker-Dimension Icon). The optical characterization of absorption spectra of the thin films in the UV–Vis region was studied using an UV–Vis spectrometer (Analytikjena SPECORD S-600). The theromogravimetric analysis of the films was carried out by using a simultaneous thermal analyzer (NETZSCH STA 409 PC). The temperature-dependent (DC) conductivity of the thin films was measured by using a

four-probe technique (Keithley 2410 Source meter) in the range 20–200°C. The AC conductivity of the thin films was measured by a tw-probe method in the frequency range 100 Hz–5 MHz using a LCR impedance analyzer (Wayne Kerr 6500 B).

RESULTS AND DISCUSSION

Scanning Electron Microscopy (SEM)

The surface morphology studied through SEM micrographs of pure PEDOT–PSS and PEDOT–PSS doped with sorbitol are represented in Fig. 1a and b. The SEM micrograph of pure PEDOT–PSS as depicted in Fig. 1a is smooth with uniform distribution of micrograins. The effect of sorbitol treatment on PEDOT–PSS results in the formation of clusters of micrograins (Fig. 1b) that are highly aggregated and interconnected forming the conducting islands. It is expected that the formation of these clusters in a polymer matrix plays an important role in the charge transport through the polymer matrix. The addition of sorbitol brings about significant change in the morphology of the pristine PEDOT–PSS films that facilitate the transport of charge carriers as well as hopping of charge carriers in the polymer backbone.

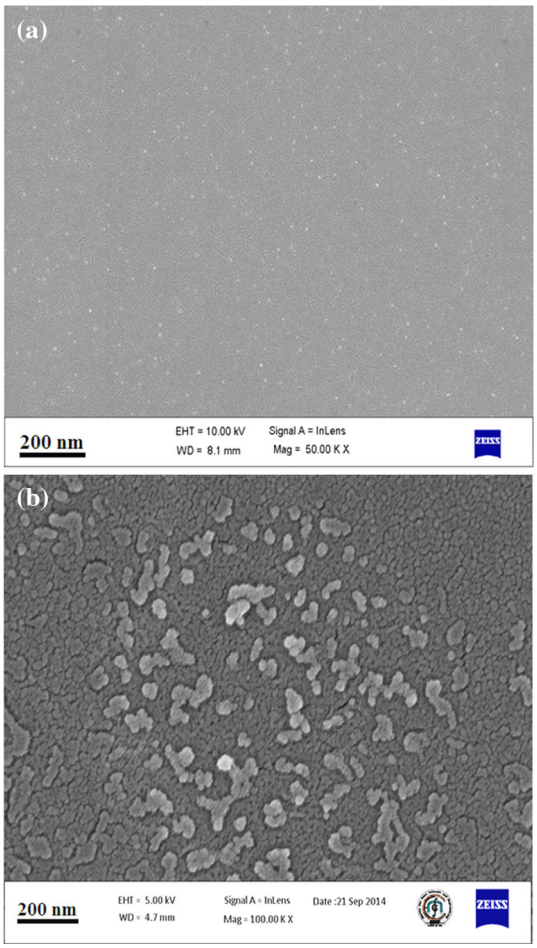

Fig. 1. SEM micrograph of (a) pure PEDOT–PSS, (b) PEDOT–PSS treated with 20 wt.% sorbitol.

Atomic Force Microscopy (AFM)

The effect of secondary doping using sorbitol on the surface morphology of PEDOT–PSS thin films was investigated using atomic force microscopy (AFM). Figure 2a and c shows the AFM height images in 2-D and 3-D for pure PEDOT–PSS, and Fig. 2b and d shows the AFM height images in 2-D and 3-D for PEDOT–PSS films treated with 20 wt.% of sorbitol. It is observed from the micrographs (Fig. 2a and c) that the addition of sorbitol results in improved phase separation between hydrophobic (bright regions) and hydrophilic (dark regions) domains as observed in the case of Nafion-doped PEDOT–PSS films.[5] The addition of sorbitol enables PEDOT and PSS clusters to rearrange in a more compact morphology as well as an increase in the size of PEDOT rich particles or clusters.[23,28] The topographic AFM images show that the films were flat with a vertical scale of nearly 5 nm for pure PEDOT–PSS and 1.5 nm for PEDOT–PSS treated with 20 wt.% of sorbitol. The addition of sorbitol increases the rms-roughness from 0.8 nm for pure PEDOT–PSS to 1.3 nm for doped PEDOT–PSS films. The increase in surface roughness may be due to the thinning effect of PSS phase that undergoes interaction with sorbitol. Sorbitol, being a polar solvent belonging to hydroxyl group, has an ability to undergo considerable interaction with PEDOT and PSS phases leading to rearrangement of PEDOT and PSS segments and formation of compact morphology. These morphological changes observed from AFM images due to the addition of sorbitol creates a better conducting path and, hence, enhances the conductivity of the sorbitol-doped PEDOT–PSS thin films.

Fourier Transform Infrared Spectroscopy (FTIR)

The FTIR spectra of pure PEDOT–PSS and PEDOT–PSS treated with sorbitol is depicted in Fig. 3. It is observed from the FTIR spectra of pure PEDOT–PSS that the characteristics peaks occur at the stretching frequency of 3500 cm^{-1} due to stretching of an O–H bond, 2900 cm^{-1} due to stretching of a C-H bond, 2500 cm^{-1} due to C=O and 2050 cm^{-1} due to stretching of a C-N bond. The sorbitol-treated PEDOT–PSS film shows a strong absorption band at 2500 cm^{-1} resulting from intrinsic vibration of a sulfoxide ion that confirms the doping of sorbitol into PEDOT–PSS. The addition of sorbitol into PEDOT–PSS results in shifting of characteristic peaks to a higher wave number as well as an increase in intensity of peaks in comparison to pure PEDOT–PSS. This provides evidence toward the formation of uniform dispersion between PEDOT–PSS and sorbitol due to strong interaction.

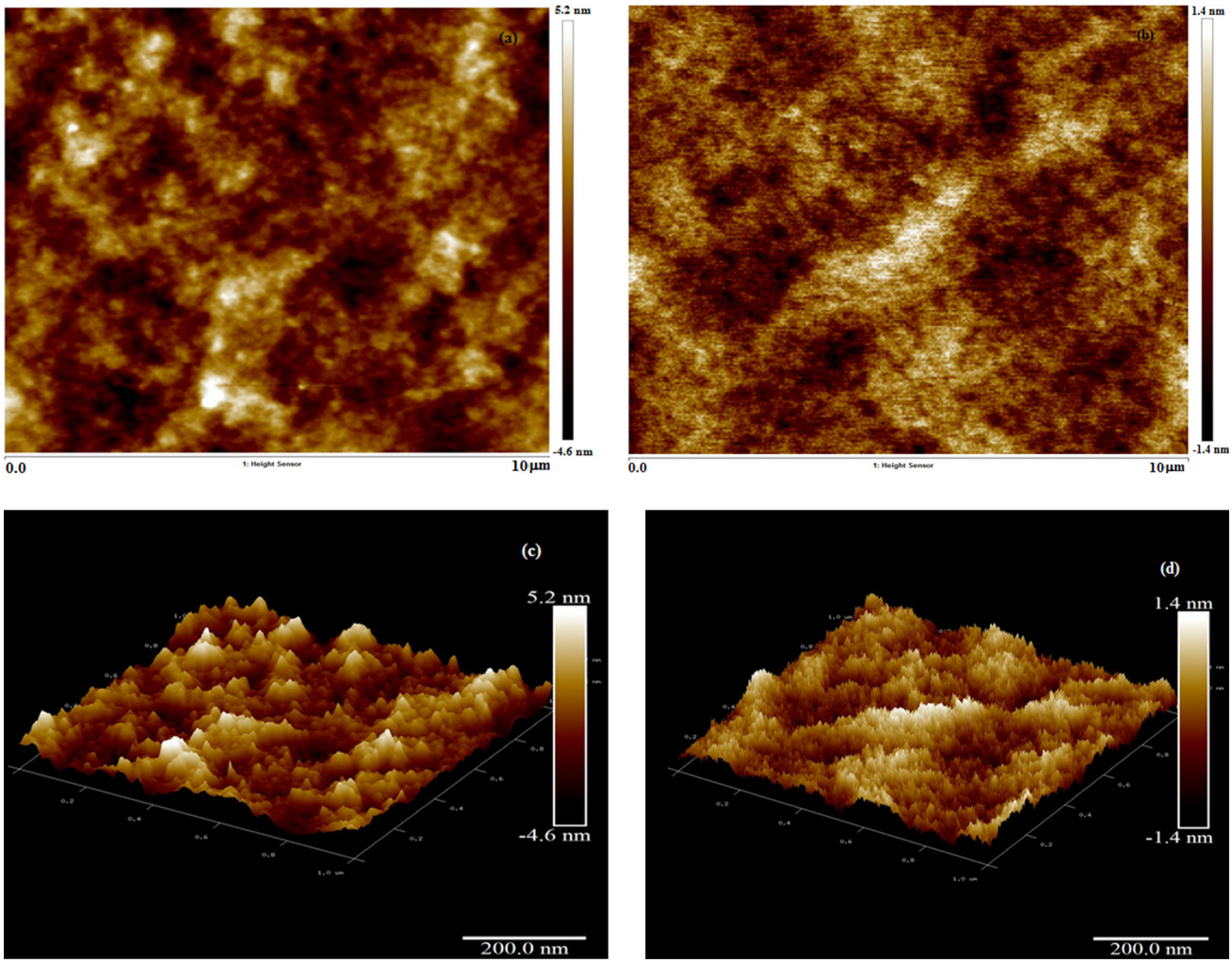

Fig. 2. AFM images of pure PEDOT–PSS and sorbitol-treated PEDOT–PSS films. (a) Pure PEDOT–PSS (2-D), (b) PEDOT–PSS treated with 20 wt.% sorbitol (2-D), (c) pure PEDOT–PSS (3-D), (d) PEDOT–PSS treated with 20 wt.% sorbitol (3-D).

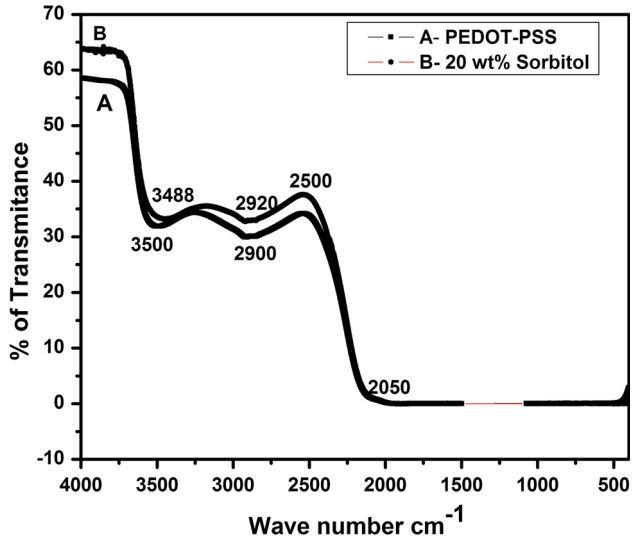

Fig. 3. FTIR spectra of pure PEDOT–PSS and sorbitol-treated PEDOT–PSS.

UV–Visible Spectroscopy (UV–Vis)

The conformational changes observed in the PEDOT–PSS matrix due to the addition of sorbitol are studied through UV–Vis spectra as shown in Fig. 4. The UV–Vis spectra for pure PEDOT–PSS and PEDOT–PSS treated with sorbitol shows similar behavior over the entire range with a sharp absorption in the UV region at 500–700 nm and a broad intense absorption close to the NIR range. The characteristic peak around 600 nm is due to higher energy transition and is due to π–π^* transitions in the PEDOT–PSS matrix. The band occurring at 900 nm represents the free carrier tail and is associated with bipolaron sub gap transition in the polymer.[29,30] A remarkable increase in the intensity of UV–Vis spectra is observed in case of sorbitol-treated PEDOT–PSS films when compared to pure PEDOT–PSS films. The observed changes in the UV–Vis spectra of pure and doped films strongly

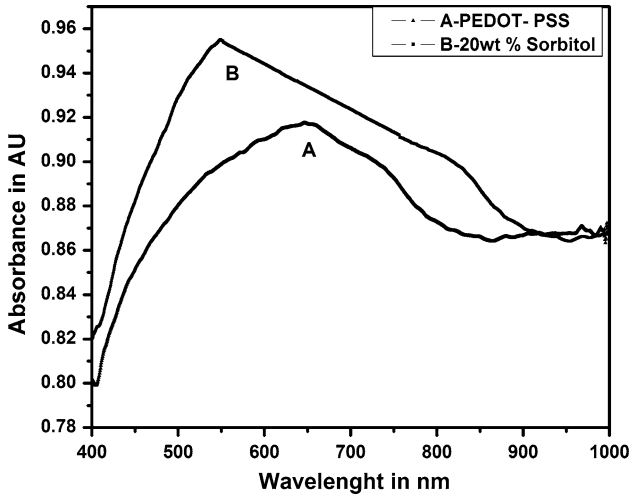

Fig. 4. UV–Vis spectra of pure PEDOT–PSS and sorbitol-treated PEDOT–PSS.

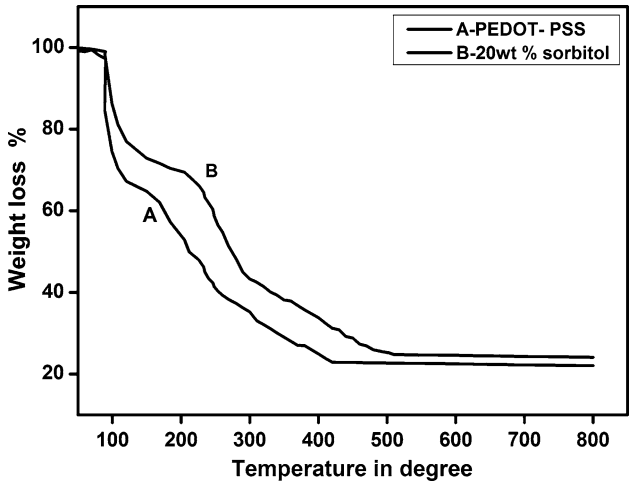

Fig. 5. TGA plots of pure PEDOT–PSS and sorbitol-treated PEDOT–PSS.

suggest the effect of sorbitol addition on the structural aspects of pure PEDOT–PSS films.

Thermo Gravimetric Analysis (TGA)

As shown in Fig. 5, PEDOT–PSS and sorbitol-treated PEDOT–PSS films were thermally characterized by using theromogravimetric analysis under nitrogen atmosphere at the heating rate of 20°C per minute. It was observed that the films exhibit 3 step weight losses. The initial weight loss at low temperatures is attributed to the evaporation of water content in the films. In the second stage the gradual weight losses are mainly due to oxidizing decomposition of the skeletal PEDOT or PSS. In the third stage at very high temperatures, a constant weight loss of 20% has been observed for both pristine and doped PEDOT–PSS films.

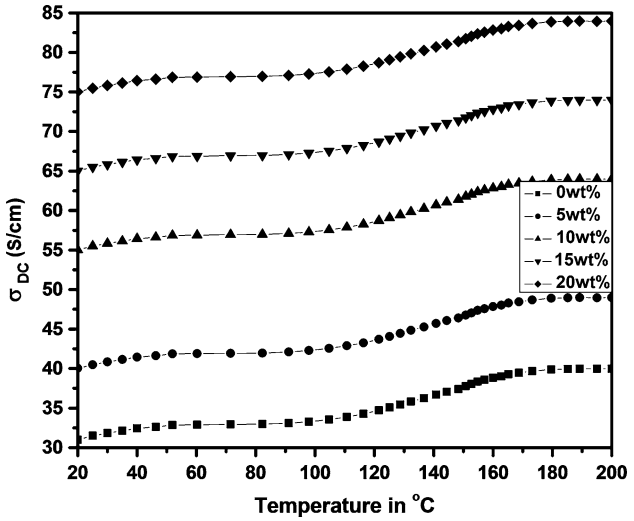

Fig. 6. Temperature-dependent conductivity of pure PEDOT–PSS and sorbitol-treated PEDOT–PSS.

Temperature-Dependent Conductivity

The effect of sorbitol content on the temperature-dependent conductivity of PEDOT–PSS film was studied in the temperature range 20–200°C. The variation of thermal conductivity for pure and sorbitol-doped PEDOT–PSS film is shown in Fig. 6. The conductivities of pure PEDOT–PSS and PEDOT–PSS doped with sorbitol shows linear 2-step variation with a slight increase in conductivity in the range 20–80°C and a rapid increase in the temperature range 80–120°C. The observed behavior is mainly due to thermally assisted conduction due to charge carrier hopping between adjacent sites. The secondary doping of sorbitol into the PEDOT–PSS matrix leads to an increase in the conductivity of sorbitol-treated films by two orders of magnitude in comparison to pure PEDOT–PSS. The conductivity enhancement of PEDOT–PSS strongly depends on the concentration of sorbitol in PEDOT–PSS as shown in Fig. 6. The conductivity change observed is mainly associated with the morphological changes in the polymer backbone due to the addition of sorbitol. The addition of sorbitol will make the coiled structures of polymer chains into linear chains that facilitate the charge carrier hopping between favorable sites that lead to increased conductivity. The addition of sorbitol into PEDOT–PSS forms the ordering of polymer chains during the film formation and driving force for the conductivity enhancement is the interaction of dipoles present in the polar solvent with the positive charges of PEDOT. The interaction between sorbitol and PEDOT–PSS through hydrogen bonding leads to the screening effect and significantly reducing the activation energies as shown in Table I. Among the different films prepared, maximum conductivity as well as better chemical stability was observed for

Table I. Activation energy (E_a) profiles

Sl. no.	Composites	Activation energy in eV
1	Pure PEDOT–PSS	4.3024123×10^{-4}
2	5 wt.%	4.1024234×10^{-4}
3	10 wt.%	3.8074125×10^{-4}
4	15 wt.%	3.5784034×10^{-4}
5	20 wt.%	3.1694102×10^{-4}

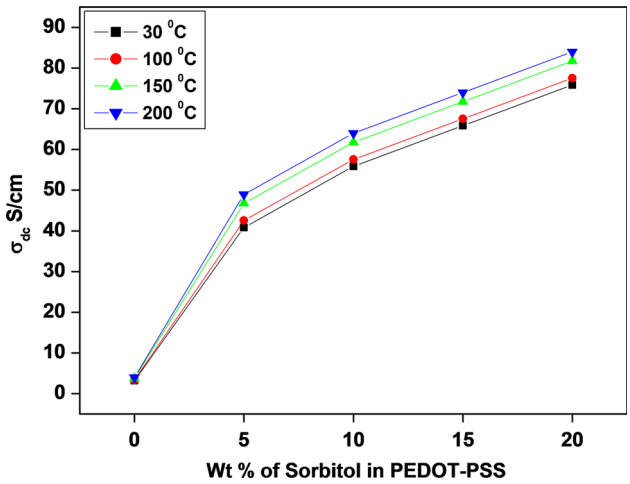

Fig. 7. Variation of DC conductivity as a function of sorbitol concentration in PEDOT–PSS.

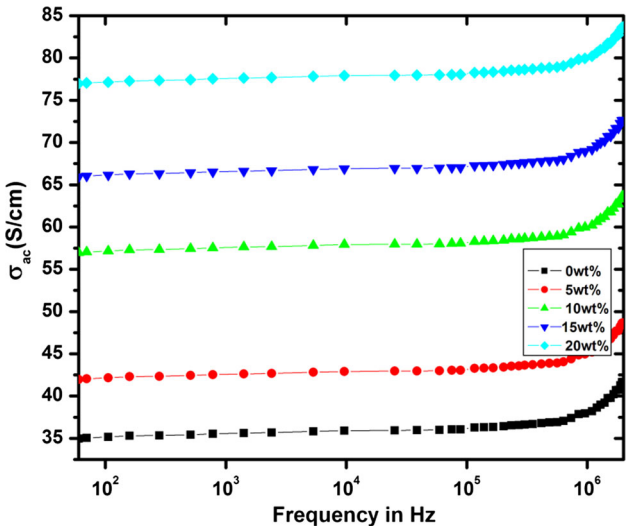

Fig. 8. Frequency dependent conductivity of pure PEDOT–PSS and sorbitol-treated PEDOT–PSS.

PEDOT–PSS films treated with 20 wt.% of sorbitol (Fig. 7).

Frequency Dependent Conductivity

The frequency-dependent conductivity of pure PEDOT–PSS and sorbitol-treated PEDOT–PSS in the frequency range 10 Hz–1 MHz is depicted in Fig. 8. Pristine PEDOT–PSS and sorbitol-treated PEDOT–PSS films exhibit similar trends of conductivity variation with increasing frequency. The conductivity of all the samples increases as per universal power law, at low frequency the conductivity is almost constant and is independent of frequency. At higher frequencies the conductivity increases with increasing frequency due to hopping conduction assisted by frequency. The addition of sorbitol in PEDOT–PSS has a strong influence on conductivity variation that depends on the concentration of sorbitol as shown in Fig. 9. The addition of sorbitol leads to an increase in conductivity of PEDOT–PSS films by two orders of magnitude. The presence of sorbitol in PEDOT–PSS enhances the grain boundary effects due to dipole polarization of segregated grains. This effect becomes maximum at the optimal concentration of 20 wt.% of sorbitol in PEDOT–PSS.

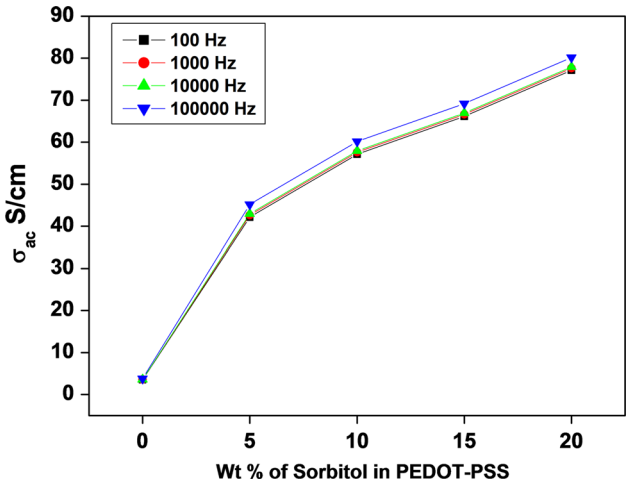

Fig. 9. Variation of AC conductivity as a function of sorbitol concentration in PEDOT–PSS.

Dielectric Studies

The frequency-dependent dielectric parameters were studied for pure PEDOT–PSS and PEDOT–PSS doped with sorbitol in the frequency range 100 Hz–5 MHz using a LCR impedance analyzer

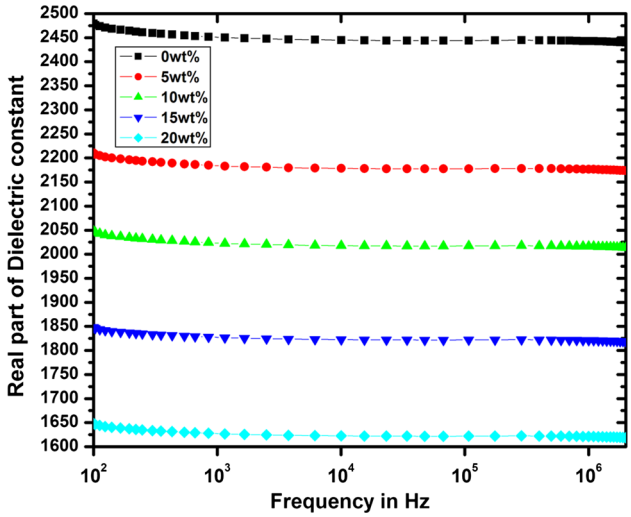

Fig. 10. Variation of the real part of the dielectric constant as a function of frequency.

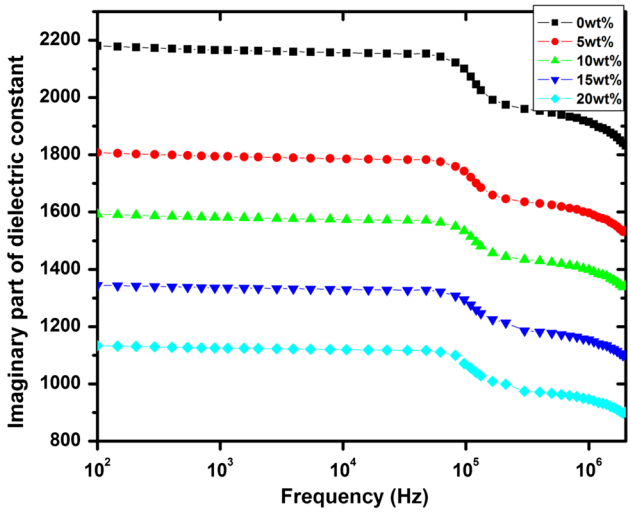

Fig. 11. Variation of the imaginary part of the dielectric constant as a function of frequency.

(Wayne Kerr 6500 B) by measuring the capacitance.[22] The real and imaginary part of the dielectric constant for pure and doped PEDOT–PSS thin films is shown in Figs. 10 and 11. It is observed from both of the figures that the dielectric constant (both real and imaginary parts) decreases with increasing frequency. From the these figures, it is observed that both components of the dielectric constant show a broad range of dispersion throughout the frequency range due to the dipole polarization associated with Maxwell–Wagner–Sillar (MWS) polarization and strong dispersion at low frequencies that mainly arises due to high conductivity. The maximum dielectric constant (both real and imaginary) is observed for pristine PEDOT–PSS, and it decreases with increasing content of sorbitol in PEDOT–PSS. Among all the samples, the 20 wt.% of sorbitol in PEDOT–PSS shows the least values of real and imaginary parts of the dielectric constant. This is mainly because of the interfacial and electrode polarization effects at the grain boundaries of PEDOT and PSS phases due to the presence of sorbitol. The presence of sorbitol leads to electrode polarization, hence, to decreases of dielectric constant (both real and imaginary parts) values.

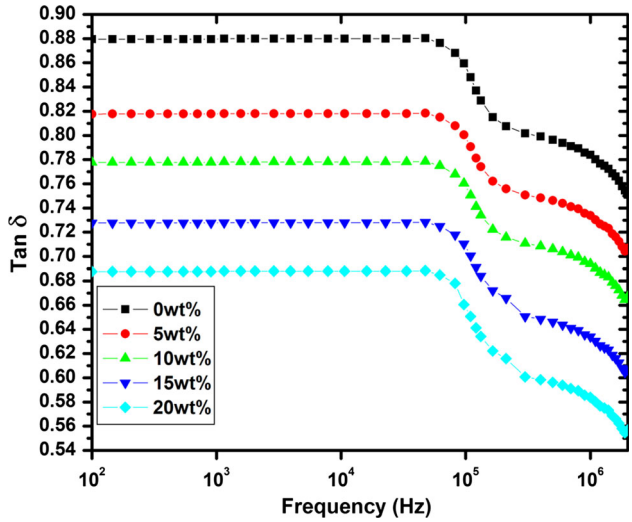

Fig. 12. Variation of dielectric loss as a function of frequency.

Figure 12 shows the variation of dielectric loss tangent as function of frequency for pristine PEDOT–PSS and PEDOT–PSS treated sorbitol. It is observed that at low frequencies the loss tangent is almost constant and frequency independent. At high frequencies there is a strong dispersion for all the samples and loss tangent values decrease sharply, and the films act as lossless materials. Among all the samples the PEDOT–PSS treated with 20 wt.% of sorbitol exhibit least values of dielectric loss which is in accordance with the variation in real and imaginary parts of the dielectric constant.

The variation of quality factor (Q) as a function of frequency is shown in Fig. 13. It is noticed that the Q value is constant in the initial stage for frequencies up to 10^3 Hz. A broad peak is observed in the frequency range 10^3–10^4 Hz, and later it becomes constant throughout the frequency range. This is mainly due to damping loss caused by the distortion of the steady state of electron flow in the polymer backbone. The Q values for all the samples are typically very small that depend on sorbitol content in the PEDOT–PSS. Among all composites, the highest value 6×10^{-4} is observed for 20 wt.%.

The frequency dependent variation of real and imaginary parts of the electric modulus (M^{I} and M^{II}) is shown in Figs. 14 and 15. From the plots it is observed that both the components of electric modulus are independent of frequency in the lower frequency region and show a strong dispersion at higher frequencies. The formation of auxiliary

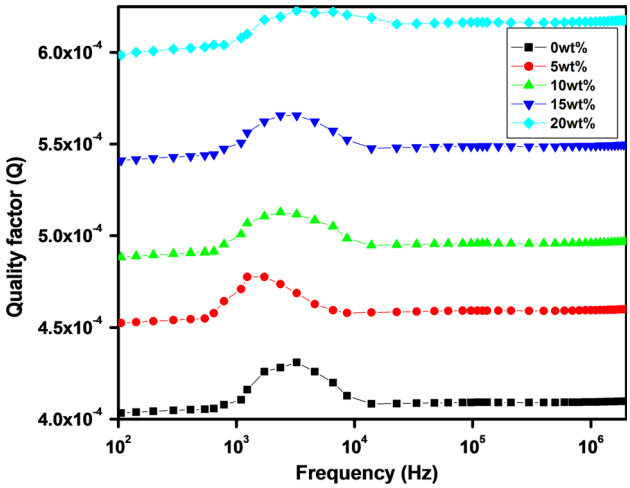

Fig. 13. Variation of quality factor as a function of frequency.

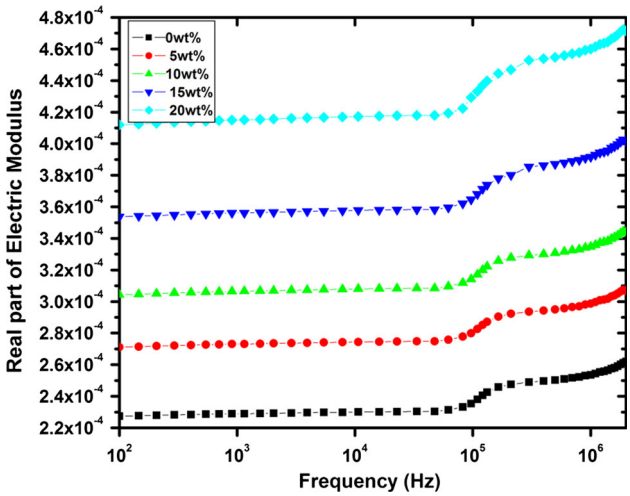

Fig. 14. Variation of the real part of the electric modulus as a function of frequency.

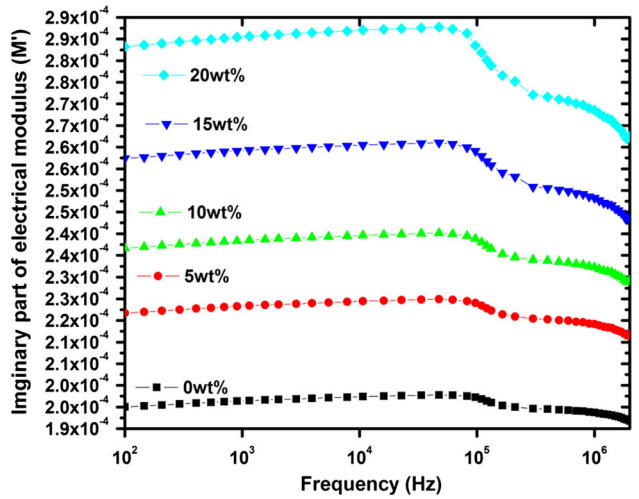

Fig. 15. Variation of the imaginary part of the electric modulus as a function of frequency.

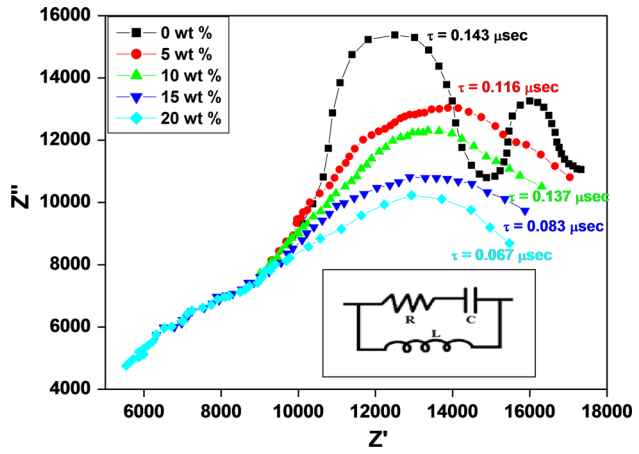

Fig. 16. Cole–Cole plots for pure PEDOT–PSS and sorbitol-treated PEDOT–PSS.

magnetic fields at the interface between the PEDOT–PSS matrix and sorbitol leads to an increase in the values of the real part and a decrease in the values of the imaginary part of the electric modulus at higher frequencies. In both the plots, films with 20 wt.% of sorbitol content show the highest values.

The impedance behavior of PEDOT–PSS and sorbitol-treated PEDOT–PSS films has been studied through impedance spectroscopy. The results are represented as a variation of the imaginary part of the impedance (Z^{II}) as a function of the real part of impedance (Z^{I}) which gives the Nyquist curves as shown in Fig. 16. When Z^{I} and Z^{II} are computed over a range of frequencies, they result in a linear region at lower frequencies and a semicircle at higher frequencies. It is observed that pure PEDOT–PSS films show double dispersion due to various relaxation mechanisms, whereas addition of sorbitol leads to formation of single dispersion at higher frequencies. It is observed from the Cole–Cole plots that the effective resistance of the sorbitol-treated PEDOT–PSS decreases when compared to pristine PEDOT–PSS films; the PEDOT–PSS treated with 20 wt.% of sorbitol shows the least resistance which is in accordance with observed conductivities (both DC and AC). The decreases in the grain resistance and surface bulk resistance for 20 wt.% of the films eventually confirmed by the low relaxation time of 0.067 μs as a result conductivity is observed to be higher compared to other compositions. The secondary doping of sorbitol into PEDOT–PSS forms an intermediate phase between PEDOT and PSS segments and impedance values depend on the grain and bulk resistance in the complex LCR circuit as shown in the inset of Fig. 16. The presence of sorbitol decreases the grain and bulk resistance of PEDOT–PSS as depicted in

the complex LCR circuit. From the equivalent circuit it can be understood that the geometrical capacitance and series resistance of the films decrease leading to an increase in conductivity values. It can also be understood from impedance measurements that the resistive behavior is more dominant and that it increases with increase in applied frequency. From the Cole–Cole plots, it also observed that there is a pronounced distribution of relaxation times for all the samples at higher frequencies that mainly depends on the concentration of sorbitol in the PEDOT–PSS matrix. This distribution in the relaxation time may be due to the charge carrier hopping between favorable sites facilitated at higher frequencies.

CONCLUSIONS

We have investigated in detail the effect of secondary doping using sorbitol on the structure and transport properties of PEDOT–PSS organic thin films. The sorbitol addition in various concentrations into the PEDOT–PSS matrix leads to significant changes in the structural and transport properties of the PEDOT–PSS thin films. Our studies reveal that addition of sorbitol causes conformational changes due to stronger interaction between the polymer backbone of PEDOT–PSS and sorbitol. These conformational changes are very well observed through FTIR and UV–Vis studies. The SEM images indicate the formation of conducting islands due to the addition of sorbitol in PEDOT–PSS. The AFM images of the thin films indicate the formation of phase separation as well as increased rms-roughness in sorbitol-treated PEDOT–PSS thin films. The increased interchain and conformational changes lead to enhancement of conductivity by two orders of magnitude as observed through DC and AC conductivities. The addition of sorbitol content into PEDOT–PSS has greater influence on dielectric parameters such as the dielectric constant, and dielectric loss as well as real and imaginary parts of the electric modulus. The Nyquist plots (Cole–Cole) shows the formation of double dispersion in the case of pristine and single dispersion for doped PEDOT–PSS films. The relaxation time in Cole–Cole plots decrease with increasing content of sorbitol; the equivalent LCR circuit for Cole–Cole plots shows a decrease in bulk resistance thus leading to enhancement of conductivity. Through this study we propose that addition of sorbitol can lead to transformation of PEDOT chains from coiled to linear structure due to dipole interactions between polar groups of sorbitol and dipoles/charges of PEDOT chains. Due to the ease in the modification of conductivities and other electrical parameters, these sorbitol-treated PEDOT–PSS thin films can be used in many technological applications towards the fabrication of optoelectronic devices.

ACKNOWLEDGEMENTS

The authors would like to acknowledge financial support for this work, from the Deanship of Scientific research (DSR), University of Tabuk, Tabuk, Saudi Arabia, under Grant No. S-123/1437.

REFERENCES

1. G. Malliaras and R. Friend, *Phys. Today* 58, 53 (2005).
2. M. Berggren and A. Richter-Dahlfors, *Adv. Mater.* 19, 3201 (2007).
3. J. DeFranco, S. Takamatsu, and G.G. Malliaras, *J. Mater. Chem.* 18, 116 (2008).
4. D.A. Bernards, D.J. Macaya, M. Nikolou, J.A. DeFranco, S. Takamatsu, and G.G. Malliaras, *J. Mater. Chem.* 18, 116 (2007).
5. X. Hou, Q. Li, T. Cheng, L. Yu, F. Wang, J. Lin, S. Dai, Y. Li, and Z. Tan, *J. Mater. Chem. A* 3, 18727 (2015).
6. J. Isaksson, P. Kjäll, D. Nilsson, N. Robinson, M. Berggren, and A. Richter-Dahlfors, *Nat. Mater.* 6, 673 (2007).
7. G. Tarabella, C. Santato, S.Y. Yang, S. Iannotta, G.G. Malliaras, and F. Cicoira, *Appl. Phys. Lett.* 97, 123304 (2010).
8. L. Groenendaal, F. Jonas, D. Freitag, H. Pielartzik, and J.R. Reynolds, *Adv. Mater.* 12, 481 (2000).
9. Y.F. Zhou, Y.B. Yuan, L.F. Cao, J. Zhang, H.Q. Pang, J.R. Lian, and X. Zhou, *J. Lumin.* 122–123, 602 (2007).
10. T.C. Tsai, W.Y. Hung, L.C. Chi, K.T. Wong, C.C. Hsieh, and P.T. Chou, *Org. Electron.* 10, 158 (2009).
11. P. Vacca, M. Petrosino, R. Miscioscia, G. Nenna, C. Minarini, D.D. Sala, and A. Rubino, *Thin Solid Films* 516, 4232 (2008).
12. C.J. Ko, Y.K. Lin, F.C. Chen, and C.W. Chu, *Appl. Phys. Lett.* 90, 3509 (2007).
13. J. Boucle, S. Chyla, M.S.P. Shaffer, J.R. Durrant, D.D.C. Bradley, and J. Nelson, *Adv. Funct. Mater.* 18, 622 (2008).
14. K.X. Steirer, M. Reese, B.L. Rupert, N. Kopidakis, D.C. Olson, R.T. Collins, and D. Ginley, *Sol. Energy Mater. Sol. Cells* 93, 447 (2009).
15. S.K.M. Jönsson, J. Birgerson, X. Crispin, G. Greczynski, W. Osikowicz, A.W.D. van der Gon, W.R. Salaneck, and M. Fahlman, *Synth. Met.* 139, 1 (2003).
16. J.Y. Kim, J.H. Jung, D.E. Lee, and J. Loo, *Synth. Met.* 126, 311 (2002).
17. S. Yoonáyang, *Chem. Commun.* 46, 7972 (2010).
18. A. Elschner and W. Lövenich, *MRS Bull.* 36, 794 (2011).
19. C.C. Oey, A.B. Djurixic, C.Y. Kwong, C.H. Cheung, W.K. Chan, M.J. Nunzi, and C. Chui, *Thin Solid Films* 492, 253 (2005).
20. J. Huang, P.F. Miller, J.S. Wilson, A.J. deMello, J.C. deMello, and D.D.C. Bradley, *Adv. Funct. Mater.* 15, 290 (2005).
21. J. Li, J. Liu, and C. Gao, *e-Polymers* 11, 428 (2011).
22. A. Pasha, A.S. Roy, M.V. Murugendrappa, O.A. Al-Hartomy, and S. Khasim, *J. Mater. Sci. Mater. Electron.* 27, 8332 (2016).
23. S. Timpanaro, M. Kemerink, F.J. Touwslager, M.M. de Kok, and S. Schrader, *Chem. Phys. Lett.* 394, 339 (2004).
24. B.Y. Ouyang, C.W. Chi, F.C. Chen, Q. Xu, and Y. Yang, *Adv. Funct. Mater.* 15, 203 (2005).
25. E. Yang, J. Kim, B.J. Jung, and J. Kwak, *J. Mater. Sci. Mater. Electron.* 26, 2838 (2015).
26. J. Li, J.-C. Liu, and C.-J. Gao, *J. Polym. Res.* 17, 713 (2015).
27. J. Ouyang, Q. Xu, C.-W. Chu, Y. Yang, G. Li, and J. Shinar, *Polymer* 45, 8443 (2004).
28. A.M. Nardes, M. Kemerink, R.A.J. Janssen, J.A.M. Bastiaansen, N.M.M. Kiggen, B.M.W. Langeveld, A.J.J.M. van Breemen, and M.M. de Kok, *Adv. Mater.* 19, 1196 (2007).
29. M. Lapkowski and A. Pron, *Synth. Met.* 110, 79 (2000).
30. S. Garreau, J.L. Duvail, and G. Louarn, *Synth. Met.* 125, 325 (2002).